J Polym Res (2013) 20:282
DOI 10.1007/s10965-013-0282-6

ORIGINAL PAPER

# Novel miscible blends of biodegradable polymer and biocompatible polyphenol acquired from natural source

**Li-Ting Lee · Ming-Chien Wu · Ming-Hsiu Lee**

Received: 13 August 2013 / Accepted: 18 September 2013 / Published online: 28 September 2013


**Abstract** A novel miscible blend of all compositions comprising biodegradable poly(butylene adipate-co-butylene terephthalate) [P(BA-co-BT)] and biocompatible tannic acid (TA) was discovered and investigated. Studies of the present work were mainly performed to discuss the miscibility and interactions of the blends. The TA/P(BA-co-BT) blends exhibit a single composition-dependent glass transition and homogeneous phase morphology, with no lower critical solution temperature (LCST) behavior upon heating to high temperature, indicating their miscibility. The $T_g$-composition relationship was proper described by the Kwei equation with moderate fitting parameters as $k=0.4$ and $q=85$. The observed heat of fusion ($\Delta H_f$) of P(BA-co-BT) revealed an obvious negative deviation from linearity with respect to the TA content, suggesting the presence of specific interactions between TA and P(BA-co-BT). Fourier-transform infrared spectroscopy (FTIR) was further conducted to identify the specific interactions. It demonstrated that the absorption of TA self-associated OH group gradually vanished and a low-frequency shift for TA phenolic-stretching band was occurred with increasing the P(BA-co-BT) content. Carbonyl-stretching bands were also resolved and were varied with the blending compositions. IR evidence reveals the existence of intermolecular hydrogen bonds in the blends, which is suggested as the main factor of the miscibility for TA/P(BA-co-BT) blends. The hydrogen bonds between TA and P(BA-co-BT) also significantly affected the behavior of nonisothermal crystallization in the blends. The nonisothermal crystallization of crystalline P(BA-co-BT) was found to be retarded by amorphous TA owing to their intimate mixing caused by noted interactions of hydrogen bonds.

L.-T. Lee (✉) · M.-C. Wu · M.-H. Lee
Department of Materials Science and Engineering, Feng Chia University, Taichung 40724, Taiwan
e-mail: ltlee@fcu.edu.tw

**Keywords** Biodegradable Polymer · Polymer Blends · Miscibility · Tannic Acid · Copolymer

## Introduction

Polymers that are mainly derived from the petroleum sources are widely applied in the daily life and investigated [1–5]. For instance, polymers can be utilized as raw materials in packing, coating, and electrical products [6–15]. Polymeric materials have high processability and diverse end-uses, but they may cause environmental pollution that results from their poor degradability under atmosphere conditions [16]. To reduce possible pollution by conventional petro-derived polymers, biodegradable polymers, which degrade more effectively, have been increasingly used in recent years. For the target to replace petro-derivative polymers by biodegradable ones, a number of biodegradable polymers/copolymers have been developed and gradually commercialized. These include poly(butylene succinate), poly(butylene succinate-co-butylene adipate) (trademark Bionolle™), poly(lactic acid) (trademark NatureWorks™), poly(3-hydroxybutyric acid) and poly(3-hydroxybutyrate-co-hydroxyvalerate) (trademark of Biopol™) [17–19]. All of these biodegradable polymers/copolymers can be degraded under atmospheric conditions or in the landfill process by micro-organisms. First, the polymer chains of these biodegradable polymers are broken into shorter parts. These are then converted into biomass or carbon dioxide and water. The products of the degradation of biodegradable polymers are normally non-toxic and do not cause significant pollution. The usage of biodegradable polymers can also reduce the use of landfills and the total amounts of generated garbage.

BASF AG (Germany) has commercialized the biodegradable copolymer of poly(butylene adipate-co-butylene terephthalate) [P(BA-co-BT)] under the trademark as Ecoflex. P(BA-co-BT) is a copolymer, rather than the general

homopolymer which has only one repeating unit on its backbone. It contains two ester repeating units on its backbone. The aliphatic butylene adipate (BA) unit on the backbone enables P(BA-co-BT) to be biodegraded to carbon dioxide and water. The other moiety, butylene terephthalate (BT), is incorporated into the polymer main chain to improve the mechanical and thermal properties of the polymer owing to its inherent functionality of aromatic structure. According to its biodegradability and favorable mechanical properties, P(BA-co-BT) has various applications and warrants further investigations. Several studies have been performed to elucidate its physical properties, and especially its crystalline behavior. Gan et al. [16] has demonstrated the solid-state structures, crystalline behavior, spherulite morphologies and thermal properties of P(BA-co-BT)s with a wide range of copolymer compositions. Additionally, Kuwabara et al. [20] and Cranston et al. [21] have utilized X-ray diffraction and solid-state $^{13}C$ nuclear magnetic resonance (NMR) to characterize the crystalline/amorphous structure and molecular mobility of P(BA-co-BT) crystallized from the melt. They suggested that butylene terephthalate units are present in both crystalline and amorphous region of P(BA-co-BT), but butylene adipate units are present only in the amorphous region. Although several studies for physical properties of P(BA-co-BT) have been performed, on a few have addressed the miscibility of P(BA-co-BT) blends. The literature includes a few studies for the miscibility of P(BA-co-BT) blends [22, 23]. The blends of poly(4-vinyl phenol)/P(BA-co-BT) [PVPh/P(BA-co-BT)] have been investigated elsewhere [23]. With hydrogen bonding interactions, PVPh and P(BA-co-BT) can form miscible blends through all blending ratios. The miscibility of P(BA-co-BT) blends must be further investigated to promote advanced applications. Specific interactions such as the hydrogen bonding interaction in the P(BA-co-BT) blends are expected to improve their miscibility or to promote the formation of a well-mixed state.

Tannic acid (TA), or tannin, is a biocompatible and biodegradable polyphenol which can be acquired from natural sources. Each TA molecule has a carbohydrate (glucose) core to which the gallic acids with phenolic structure are bonded. TA can be extracted naturally from either plants or microorganisms and it has medicinal/pharmacological end-uses. Its particular biological features such as biocompatibility and biodegradability will support more advanced applications in the near future. The interactions between TA and other polymers have been proven to enable TA to bind with biopolymers such as collagen, gelatin, albumin and polysaccharide through noncovalent interactions [24–27]. Hydrogen bonding interactions between TA and polymers that contain proton-accepting functional groups such as ester and ether groups have been characterized [28]. Effective mixing state via interactions between TA and polymeric materials is expected to further improve the biological properties of the formed blends.

In this study, blends of biodegradable P(BA-co-BT) and the natural bioresourceful TA were investigated. The present work was mainly performed to discuss the miscibility and interactions of the TA/P(BA-co-BT) blends. P(BA-co-BT) is a biodegradable polymer and is commercialized as an environmental friendly material with the purpose of substituting the petro-source polymers. Blending P(BA-co-BT) with other materials can further tune the properties of P(BA-co-BT) and broaden the applications of P(BA-co-BT). TA is a natural polyphenol that can be acquired from tea or plant leaves. The phenolic groups of TA can be adopted as proton-donating groups to induce hydrogen bonding interactions in the blends. To blend TA with P(BA-co-BT), hydrogen bonding interactions are expected to be introduced in the blends by the proton-donating groups of TA and the proton-accepting groups (carbonyl groups) of P(BA-co-BT). These specific interactions in the blends could effectively enhance the miscibility and the mixing among the molecules. In the well-mixed or miscible states, the versatility of the end-use for biodegradable/biocompatible TA/P(BA-co-BT) blends would be further increased, with widening their range of applications as multi-functional biomaterials.

## Experimental

### Materials and preparation

Tannic acid (TA with $M_w$=1721 g/mol) was supplied from Sigma-Aldrich Co., and was used without further purification. P(BA-co-BT) was obtained from BASF AG (Germany), with a commercial name Ecoflex®, $M_w$=135,000 g/mol; $T_g$~−45 and $T_m$~124 °C (measured with differential scanning calorimetric (DSC)), and density=1.27 g/cm$^3$. The copolymer's relative molar fractions as determined by $^{13}C$ solid-state cross-polarization/magic angle spinning NMR is 56 mol% BA and 44 mol% BT [21]. A solution-blending procedure was adopted for sample preparation. Polymers in *p*-dioxane solutions (4 wt.%) of different P(BA-co-BT) to TA ratios were prepared and then cast onto either glass or aluminum substrates at 45 °C for 48 h. Afterwards, the as-cast films were moved to a vacuum oven with temperature control at 80 °C for 4 days in order to remove residual solvent before measurements.

### Apparatus and procedures

*Optical microscopy (OM)* An Olympus CX41 optical microscope (OM) equipped with a charge-coupled device digital camera and a Linkam THMS-600 microscopic heating stage with TP-95 system controller was used to observe the phase behavior of blending samples. Solution-blended samples for OM study were solution-coated on glass substrate, covered with top glass, and pressed into films of proper thickness (ca. 10~15 μm). For the

observation, all samples were first fast heated to the temperature above the $T_m$ of P(BA-co-BT) (150 °C) to melt the crystallites caused by sample preparation. Samples were then gradually heated by a rate of 2 °C/min. Carefully observations for the phase behavior and the possible phase transition caused by the elevation of temperature were made in this study.

*Differential scanning calorimetry (DSC)* Thermal analysis and measurements for $T_g$'s of the blends were performed using Perkin-Elmer DSC-8500 equipped with a mechanical intracooler under dry nitrogen purge. Scanning rates were 20 °C/min and the reported $T_g$ values were taken as the onset of the glass transition. All samples were pressed to flat films to ensure good thermal conduction and temperature distribution. Amorphous specimens by premelting/quenching treatment were used for the characterization of glass transition temperature. After the experiments, obtained $T_g$ values were plotted against the blends' compositions to investigate the $T_g$-composition relationships of the blends. For the discussions of nonisothermal crystallization, all blending specimens were first melted at 150 °C to destroy thermal history and then cooled at different cooling rates to enable the investigations on nonisothermal crystallization.

*Fourier-transform infrared spectroscopy (FT-IR)* Fourier-transform infrared spectroscopy (FT-IR; Perkin-Elmer Frontier™) was used to identify the state of molecular interactions between P(BA-co-BT) and TA. All spectra were recorded at a resolution of 4 $cm^{-1}$ with an accumulation of 64 scans in the range of 400~4,000 $cm^{-1}$. TA, P(BA-co-BT) and their blends were solution-cast as thin and uniform films from 2~4 wt.% solutions directly onto KBr pellets at 45 °C. Subsequently, vacuum-dried samples were then subjected to IR measurement at ambient temperature.

*Scanning electron microscopy (SEM)* Blend samples were also examined using a scanning electron microscope (SEM, model: Hitachi S3000) to observe the phase morphology for greater magnification. Blend films for SEM observation were solution-cast to be thick enough so that fracture surface of the thickness (cross section) could be conveniently examined. Before SEM observation, the fractured blend samples were coated with gold by vapor deposition using vacuum sputtering.

## Results and discussion

### Microscopic characterization of TA/P(BA-co-BT) blends

Optical microscopy (OM) was firstly utilized in the morphological characterization. Figure 1 shows the OM results for TA/P(BA-co-BT) blends with the compositions: (a) 50/50 and (b) 70/30. In general, well-mixed or miscible blends exhibit homogeneous phase morphology as revealed by the "optical clear" OM images that they would generate. The OM results in Fig. 1 demonstrate that all blends have the same morphological type, as they yield optically clear images with 800x magnification. No distinct phase-separated domain can be resolved by OM. At the resolution of OM, blends of TA and P(BA-co-BT) examined in this study can be preliminarily identified as miscible blends with no distinct phase separation. Notably, OM characterizations were also performed over the entire compositional range of TA/P(BA-co-BT) blends. All of the compositions yielded a similar result, showing homogeneous phase morphology without any phase separation for TA/P(BA-co-BT) blends. To further investigate whether the blends exhibited the "Lower Critical Solution Temperature" (LCST) behavior, all specimens were subjected to heat from room temperature to 250 °C. Figure 2 displays the OM results for TA/P(BA-co-BT)=50/50 blend that were recorded at different temperatures, which were (a) room temperature, (b) 100 °C, (c) 180 °C, and (d) 250 °C. The results of Fig. 2 demonstrate that the specimen yields only optically clear image (without heterogeneous phase separation). Therefore, as the temperature is increased at a controlled heating rate of 2 °C/min, no phase-separated morphology is induced. Experiments were also performed on various compositions of TA/P(BA-co-BT) blends. As the temperature was increased from room temperature to 250 °C, only homogeneous phase morphology was observed. Preliminary OM characterization indicates that TA/P(BA-co-BT) blends are all miscible without detectable phase separation under the resolution of OM. Additionally, as the temperature is gradually increased, the blends exhibit no LCST phase behavior as determined using OM.

Scanning electron microscopy (SEM) can provide high-resolution image to elucidate phase morphology. It was also applied to study the TA/P(BA-co-BT) blends. SEM images with high magnification were obtained and the phase morphology of the TA/P(BA-co-BT) blends was finely resolved. The fracture surfaces of fractured samples were observed using SEM. Typical SEM results for the TA/P(BA-co-BT)=50/50 blends are discussed herein. Figure 3 presents SEM images of the TA/P(BA-co-BT)=50/50 blend under the following conditions: (a) as-cast, (b) annealed at 100 °C for 2 mins and then quenched, (c) annealed at 180 °C for 2 mins and then quenched, and (d) annealed at 250 °C for 2 mins and then quenched. Notably, the annealing/quenching of the sample is carried out to freeze its phase morphology at a specific annealing temperature to enable observation. As displayed in Fig. 3, SEM reveals a homogeneous morphology rather than the morphology with phase separation, indicating that the as-cast blend and the blends annealed at various temperatures are miscible and lack of temperature-induced phase separation. Both OM and SEM characterizations were conducted, and the

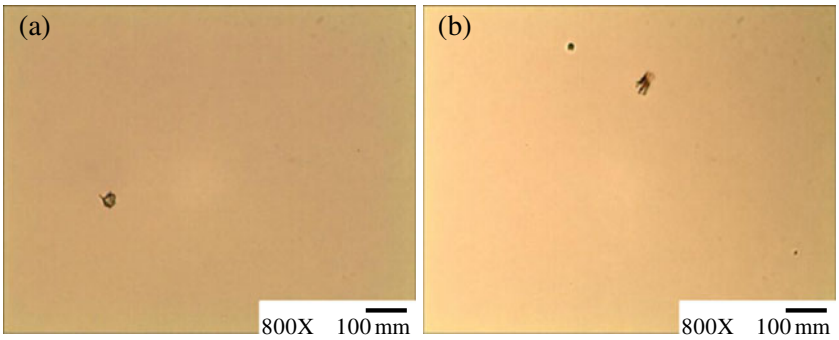


**Fig. 1** OM results for TA/P(BA-co-BT) blends with the compositions: **a** 50/50 and **b** 70/30

results suggest that the TA/P(BA-co-BT) blends are miscible without any phase separation with obvious domains. The blends also do not exhibit the LCST behavior that accompanies temperature-induced phase separation. The miscibility of TA/P(BA-co-BT) blends will be further clarified by the studies of differential scanning calorimetry (DSC) as follows.

DSC to determine miscibility of TA/P(BA-co-BT) blends

The DSC single $T_g$ criterion for identifying miscible blends was adopted to study the miscibility of TA/P(BA-co-BT) blends herein. Figure 4 shows DSC thermograms of P(BA-co-BT)/TA blends with varying compositions, as indicated in the figure. The melting/quenching treatment by DSC was conducted to avoid the initial crystallinity of P(BA-co-BT). Blending samples were first melted at the temperature just above P(BA-co-BT)'s $T_m$ and then quenched for DSC measurements. Figure 4 shows the sequential scan after melting/quenching each sample. In Fig. 4, it displays only one single $T_g$ for each of the TA/P(BA-co-BT) blends with various compositions, proving that the TA/P(BA-co-BT) blends with any compositions are miscible. The intimately mixing of TA and P(BA-co-BT) at the molecular level is suggested. Even though TA is not the high molecular weight polymer that undergoes successive covalent bonding on the backbone, the intra-molecular hydrogen bonds among the hydroxyl groups of TA may provide the stable interactions that form supra-molecular TA with a detectable $T_g$ for the DSC thermogram transition (with an onset at 38 °C). Some bisphenol molecules have been reported to exhibit a similar phenomenon [29]. The $T_g$-*v.s.*-composition relationship of TA/P(BA-co-BT) blends is also studied. The composition-dependent $T_g$ can be normally described by various equations. Taking into account the free volume and the thermal expansion of the blends, the Gordon-Taylor equation [30], which is presented below as Eq. (1), is generally fitted to the $T_g$-*v.s.*-composition relationship.

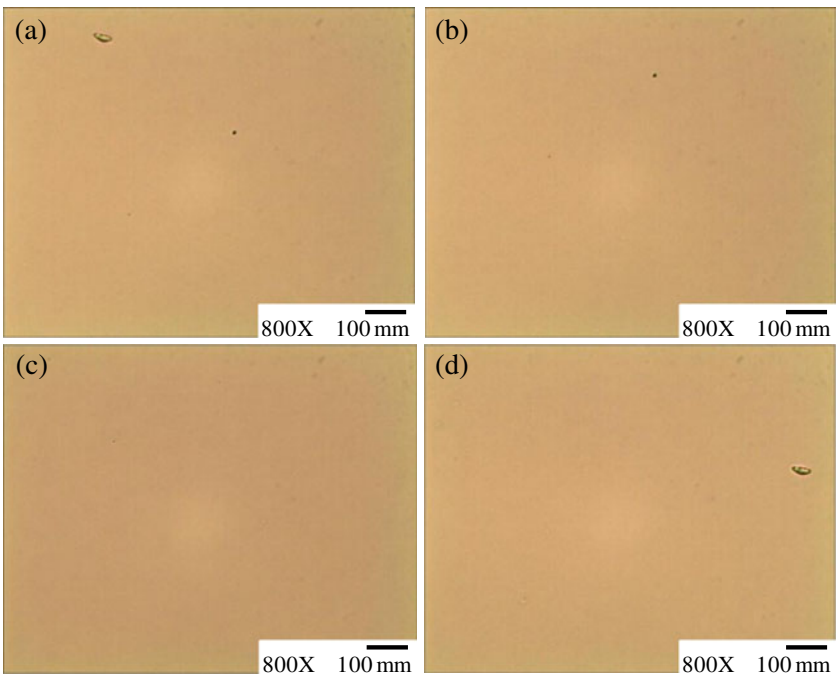


**Fig. 2** OM results for TA/P(BA-co-BT)=50/50 blend that were recorded at different temperatures, which were **a** room temperature, **b** 100 °C, **c** 180 °C, and **d** 250 °C

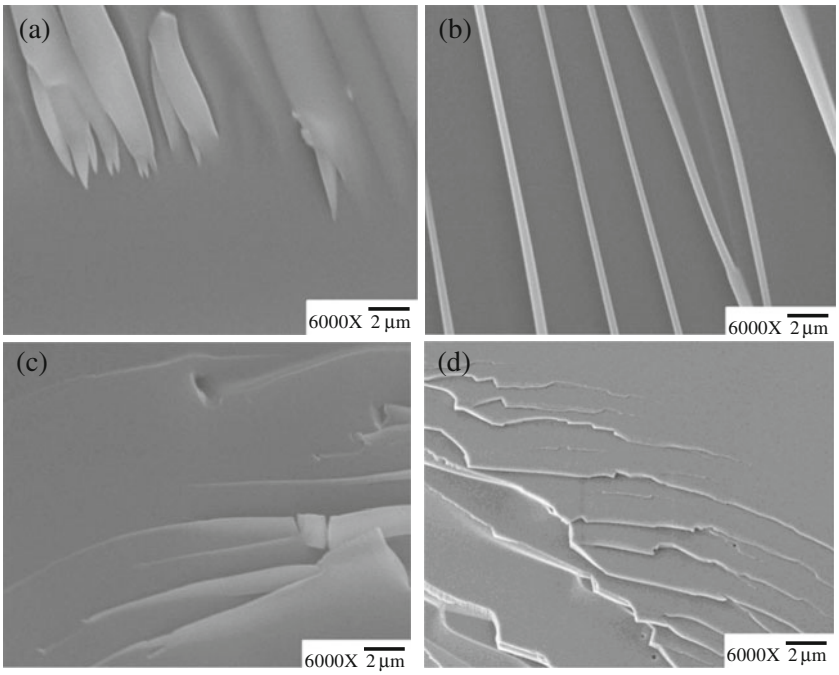


**Fig. 3** SEM images of the TA/P(BA-co-BT)=50/50 blend under the following conditions: **a** as-cast, **b** annealed at 100 °C for 2 mins and then quenched, **c** annealed at 180 °C for 2 mins and then quenched, and **d** annealed at 250 °C for 2 mins and then quenched

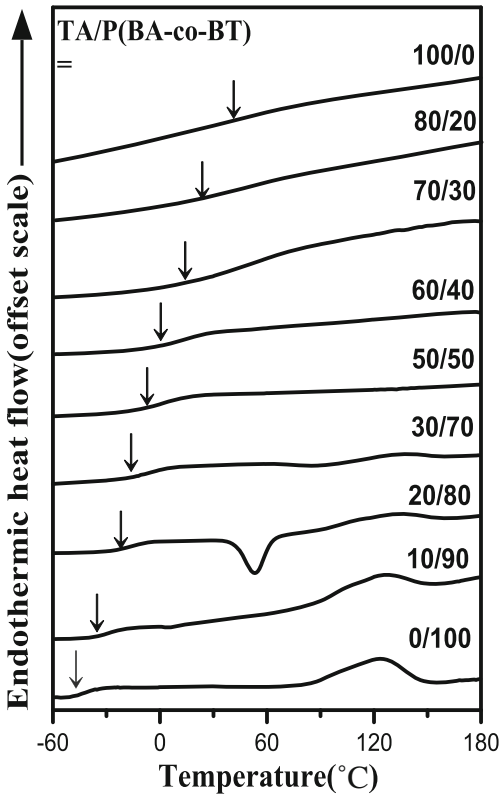


**Fig. 4** DSC thermograms of P(BA-co-BT)/TA blends with varying compositions

$$T_g = \frac{w_1 T_{g1} + k w_2 T_{g2}}{w_1 + k w_2} \quad (1)$$

where $w_1$ and $w_2$ are the weight fractions of the components in the blends, $T_{g1}$ and $T_{g2}$ represent the corresponding glass transition temperatures, and k is the fitting parameter. Furthermore, to deal with the influence of specific interactions such as the hydrogen bonding interactions on the $T_g$-*v.s.*-composition relationship, Kwei et al. modified the conventional Gorden-Taylor equation. A term to represent the influence of specific interactions on the $T_g$-*v.s.*-composition relationship was added:

$$T_g = \frac{w_1 T_{g1} + k w_2 T_{g2}}{w_1 + k w_2} + q w_1 w_2 \quad (2)$$

The Kwei equation [31] as Eq. (2) is obtained by modifying the Gorden-Taylor equation with including a term of $qw_1w_2$. The parameter q is defined to represent the strength of specific interactions in the blends. The $T_g$-*v.s.*-composition relationship for the blends with specific interactions such as the hydrogen bonding interactions can be adequately described by the Kwei equation. The $T_g$ values of TA/P(BA-co-BT) blends are replotted again with respect to the TA content. Figure 5 reveals the $T_g$-*v.s.*-composition relationship for TA/P(BA-co-BT) blends. Both the Gorden-Taylor equation and the Kwei equation are fitted to the experimental data. As shown in Fig. 5, the Kwei equation ($k$=0.4, $q$=85) provides the better fit. The results of Fig. 5 suggests that the specific interactions are present between TA and P(BA-co-BT) in the blends. As suggested by Coleman et al. [32], the parameter "q" may be influenced by the balance between the original

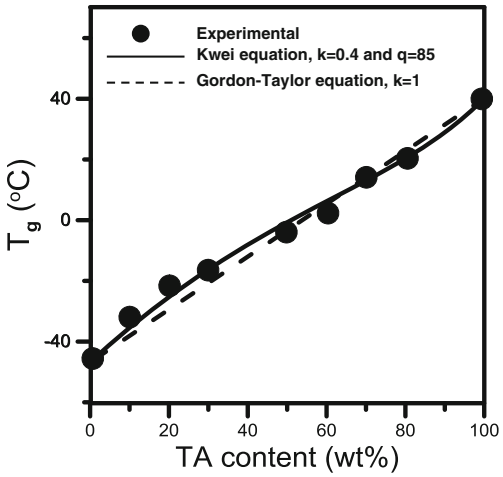


**Fig. 5** $T_g$-*v.s.*-composition relationship for TA/P(BA-co-BT) blends

intramolecular hydrogen bonding interactions (in neat TA) and the newly formed intermolecular hydrogen bonding interactions (between TA and P(BA-co-BT)). For the TA/P(BA-co-BT) blends, the positive q value of 85 is believed to be attributable to the specific interactions between TA and P(BA-co-BT) which cause the two constituents to mix intimately at a molecular level, forming the miscible blends that are identified by microscopy and DSC. Figure 6 shows the heat of fusion ($\Delta H_f$) as a function of TA content (wt%) in the blends. Note that P(BA-co-BT) is the only crystallizable component in the blends. The other component, TA, is inherently amorphous and is non-crystallizable. The values of $\Delta H_f$ were calculated by the area of melting transition from DSC traces in Fig. 4 and were normalized by the weight fractions of P(BA-co-BT) in the blends. In Fig. 6, the closed circles are demonstrated for the $\Delta H_f$ values with different compositions in the blends. In addition, the solid line in Fig. 6 describes the tendency change of the $\Delta H_f$ values with varying blending

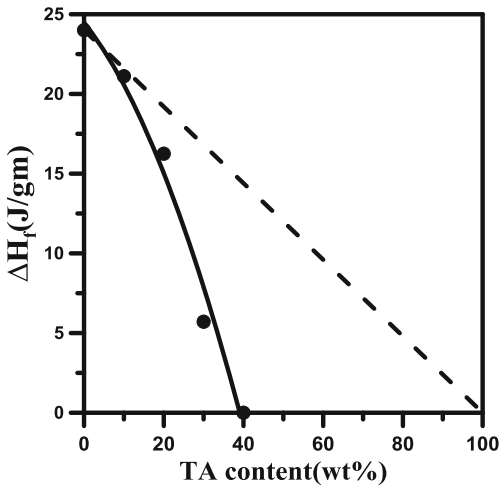


**Fig. 6** The heat of fusion ($\Delta H_f$) as a function of TA content (wt%) in TA/P(BA-co-BT) blends

compositions. The linear relationship between the $\Delta H_f$ values and the compositions is also displayed as the dashed line in Fig. 6. As shown in Fig. 6, the blends show decreasing $\Delta H_f$ on increasing the TA content. In addition, the observed $\Delta H_f$ reveals an obvious negative deviation from linearity with respect to the TA content in the blends. The dependence of the enthalpy of transitions on blend composition could provide additional evidences of the intermolecular interactions in the blends [33]. Normally, a blend's heat of fusion presenting linear dependence on blend composition infers either weak interactions or no intermolecular interactions with phase separation; on the other hand, a significant negative deviation from linearity suggests the disruption of the crystallizing polymer chains by the interacting non-crystalline components. Figure 6 provides additional evidences for the existence of intermolecular interactions between TA and P(BA-co-BT), and the noted interactions can effective lead to the formation of miscible blends of TA and P(BA-co-BT), as characterized by OM, SEM and DSC single $T_g$ criterion. Further studies of the specific interactions in the blends will be conducted using FTIR spectroscopy.

## IR spectroscopic determination of interactions in TA/P(BA-co-BT) blends

OM, SEM and DSC analyses demonstrated that the blends of TA/P(BA-co-BT) are miscible with homogeneous phase behavior. Although interactions that are caused by hydrogen bonds can be expected to occur between the hydroxyl functional group of TA and the carbonyl group of P(BA-co-BT), relative study is required for confirmation. FTIR characterization was performed to identify the interactions between TA and P(BA-co-BT). Figure 7 presents the FTIR spectra in the hydroxyl-stretching region for TA/P(BA-co-BT) blends with different compositions. The IR absorption peaks of the –OH groups in TA are observed at 3360 and 3206 $cm^{-1}$, and are related to the free and self-associated (intramolecular hydrogen bonds) –OH groups, respectively. As the P(BA-co-BT) content in the blends increases, the intensity of the self-associated band declines, reflecting corresponding increase in the strength of the intermolecular hydrogen bonding interactions between TA and P(BA-co-BT). This result suggests that the interaction state in the blends gradually changes as the P(BA-co-BT) content in the blends is increased from low to high, since the original intramolecular hydrogen bonds in neat TA are broke and new intermolecular hydrogen bonds are formed between TA and P(BA-co-BT). Other polyester blends with TA have exhibited a similar phenomenon [28, 34]. The phenolic C-O stretching band of TA was also analyzed to examine the hydrogen bonding interactions in the blends. The peaks that are related to the phenolic C-O stretching band of TA may be affected by its specific interactions with P(BA-co-BT) via hydrogen bonds. Figure 8 shows the FTIR spectra

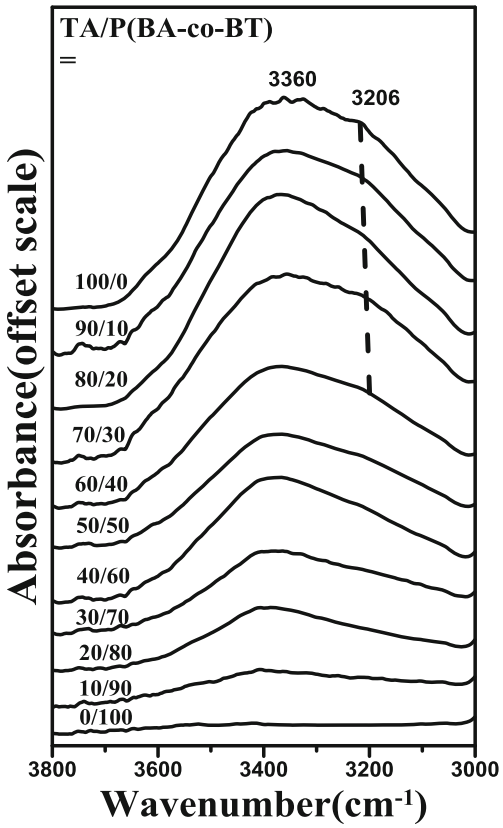


**Fig. 7** FTIR spectra in the hydroxyl-stretching region for TA/P(BA-co-BT) blends with different compositions

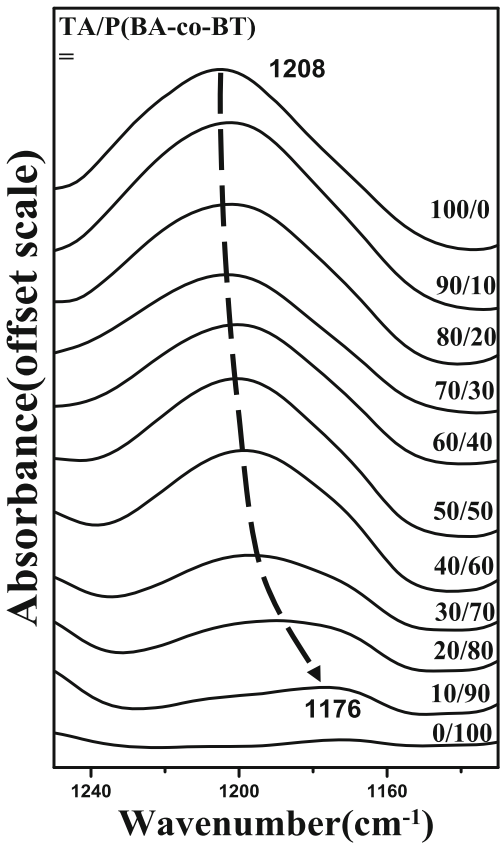


**Fig. 8** FTIR spectra in the phenolic C-O stretching region for TA/P(BA-co-BT) blends with different compositions

in the phenolic C-O stretching region for TA/P(BA-co-BT) blends with different compositions. The phenolic C-O stretching vibration of TA yields a sharp peak at 1208 $cm^{-1}$. The figure demonstrates that the peak at 1208 $cm^{-1}$ gradually shifts to a lower wavenumber of 1176 $cm^{-1}$ as the P(BA-co-BT) content increases to 90 wt.%. Such low wavenumber shifting further reveals specific interactions occur between TA and P(BA-co-BT), which may be attributed to the hydrogen bonding interactions between TA and P(BA-co-BT). In an earlier study of TA/PCL blends, similar phenolic C-O spectra were also obtained owing to the presence of intermolecular hydrogen bonding interactions in the blending system [28]. The spectroscopic evidence of band shifting in the phenolic C-O stretching region (by 32 $cm^{-1}$ from 1208 $cm^{-1}$ to 1176 $cm^{-1}$) further confirms the presence of specific interactions in the blends. The hydrogen bonding interactions are proven to exist between the proton-donating TA and the proton-accepting P(BA-co-BT). Figure 9 displays the carbonyl stretching region in FTIR spectra of TA/P(BA-co-BT) blends with different compositions. In Fig. 9, the absorption peak of neat TA is found at 1718 $cm^{-1}$. The IR carbonyl stretching region of neat P(BA-co-BT) exhibits two (partially overlapping) doublet bands, which are associated with the peak at 1731 $cm^{-1}$ and another close peak at 1715 $cm^{-1}$. It can find that the carbonyl stretching band of TA and that of P(BA-co-BT) vary with the relative compositions of the blends. Additionally, Fig. 9 also suggests that the absorption band of TA and that of P(BA-co-BT) could overlap with each other at IR carbonyl stretching region. The similar feature of IR carbonyl stretching band was also found in the miscible blends of TA and polyester with the carbonyl functional group [34].

## Influence of specific interactions on nonisothermal crystallization of TA/P(BA-co-BT) blends

The behavior of nonisothermal crystallization was also investigated for the blends. It was performed to discuss whether the specific interactions between TA and P(BA-co-BT) would influence the nonisothermal crystallization of P(BA-co-BT) in the blends. Blending samples were subjected to melting/cooling processes with different cooling rates for nonisothermal crystallization. Figure 10 shows the DSC results of nonisothermal crystallization with different cooling rates for (a) neat P(BA-co-BT), (b)TA/P(BA-co-BT)=10/90, and (c) TA/P(BA-co-BT)=20/80. It should note that for the TA/P(BA-co-BT) blends with TA=30 wt.% or greater, the blends are no longer

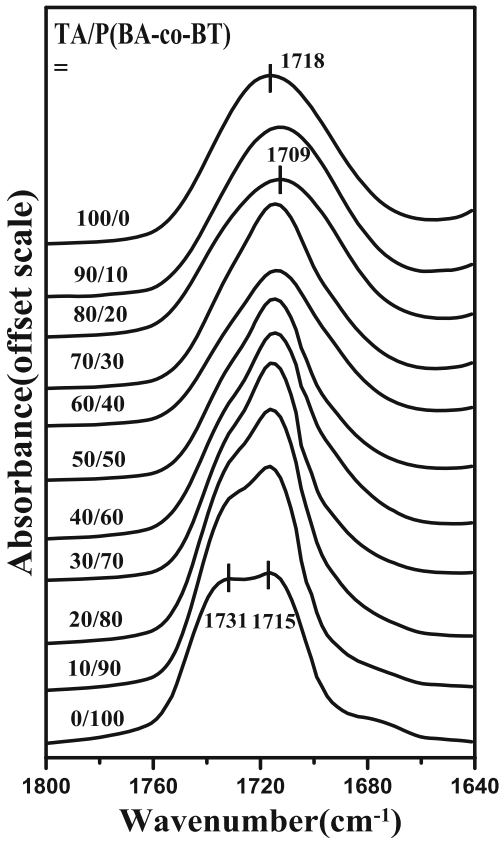


**Fig. 9** Carbonyl stretching region in FTIR spectra of TA/P(BA-co-BT) blends with different compositions

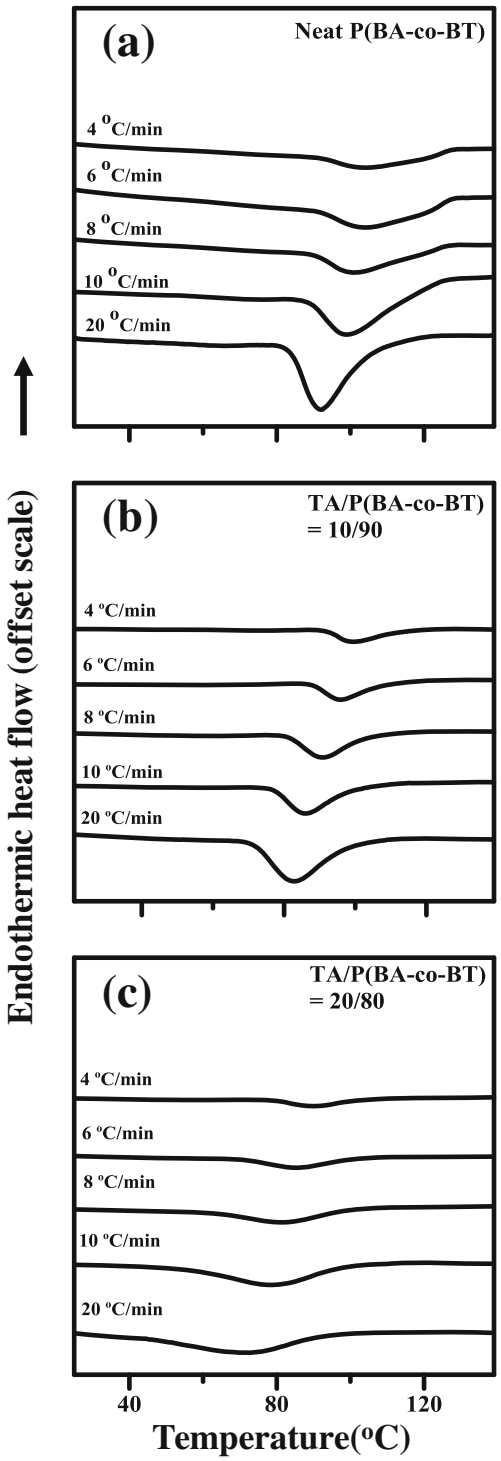


**Fig. 10** DSC results of nonisothermal crystallization with different cooling rates for **a** neat P(BA-co-BT), **b** TA/P(BA-co-BT)=10/90, and **c** TA/P(BA-co-BT)=20/80

crystallizable under nonisothermal crystallization, and their results of noisothermal crystallization cannot be discussed. For further discussions, the values of peak temperature ($T_p$) and the values heat of nonisothermal crystallization ($\Delta H_{n,c}$) for all samples were analyzed. Figure 11 (a) presents a plot of $T_p$-*v.s.*-TA content in the blends with different cooling rates of nonoisothermal crystallization. Additionally, Fig. 11 (b) shows a plot of $\Delta H_{n,c}$-*v.s.*-TA content in the blends with different cooling rates of nonisothermal crystallization. From the results of Fig. 11 (a), it can find that at the same cooling rate for different samples, the peak temperature ($T_p$) is shifted to lower temperature values as the content of TA increases in the blends, which infers that the addition of amorphous TA in the blends would significant influence the nonisothermal crystallization of the blends. The increase in TA content is suggested to inhibit the nonisothermal crystallization of P(BA-co-BT) in the blends. In addition, it also shows a similar tendency for the heat of nonisothermal crystallization ($\Delta H_{n,c}$). In Fig. 11 (b) at a fixed cooling rate, it shows that the $\Delta H_{n,c}$ value is decreased as the amount of TA increases in the blends. In summary, TA can efficiently interact with P(BA-co-BT) by hydrogen bonding interactions to cause miscible molten state. Nonisothermal crystallization of P(BA-co-BT) in the blends, which is initiated from miscible melt and subsequently processed by cooling down to lower temperature, is suggested to be affected by the hydrogen bonding interactions between TA and P(BA-co-BT) in the

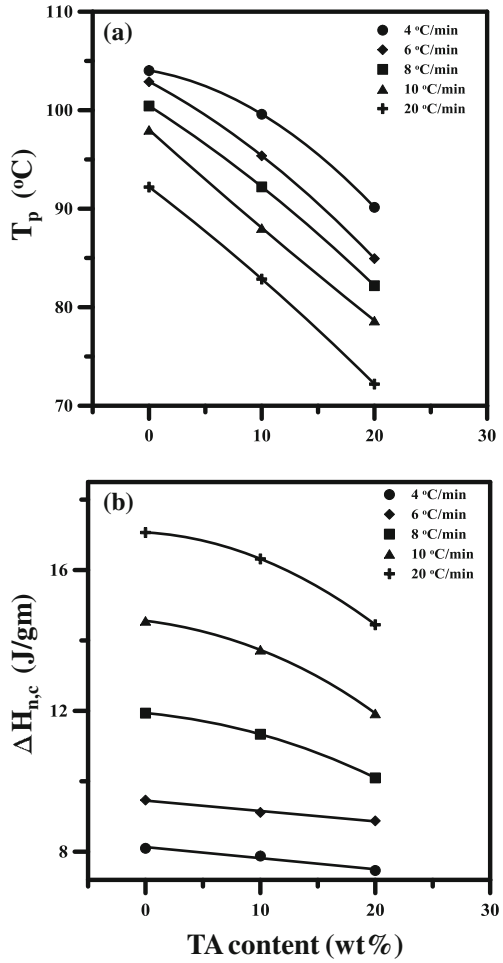


**Fig. 11** **a** Plot of $T_p$-*v.s.*-TA content in the blends with different cooling rates; and **b** Plot of $\Delta H_{n,c}$-*v.s.*-TA content in the blends with different cooling rates

blends. Nonisothermal crystallization of the crystalline P(BA-co-BT) can be obviously retarded, and even suppressed, by the amorphous component of TA in the blends with the specific interactions as hydrogen bonds.

## Discussions on interaction states of miscible TA/P(BA-co-BT) blends

To develop a novel material for advanced applications, blends of TA and P(BA-co-BT) were prepared. TA and P(BA-co-BT) are biocompatible and biodegradable. TA can also be obtained from natural sources as natural polyphenol, giving it a unique advantage for use in green science. Blends of TA and P(BA-co-BT) can be further utilized in the production of novel bio-related materials and they have applications that support the development of green technology. Figure 12 presents the interaction states of the miscible TA/P(BA-co-BT) blends in this study. By proper illustration, further discussions are made to clarify the interaction states of miscible TA/P(BA-co-BT) blends characterized in this study. Blends of TA and P(BA-co-BT) are miscible, as determined by DSC, OM and SEM. Self-associated and inter-associated hydrogen bonding interactions are also identified by FT-IR. The type I interaction state in the figure presents the pseudo-polymer in which most of the TA molecules are connected with each other by self-associated hydrogen bonding interactions. This supra-molecular TA (pseudo-polymer type) with self-associated hydrogen bonding interactions does not only present general small molecular behavior but also shows some inherent properties of normal polymer, including a thermo-transition $T_g$ in the DSC thermogram. Type II interaction state exhibits inter-associated hydrogen bonds between proton-donating TA and proton-accepting P(BA-co-BT), enabling the formation of miscible blends of TA and P(BA-co-BT). The higher-$T_g$ TA with a supra-molecular structure (pseudo-polymer type) is intimately mixed with the lower-$T_g$ P(BA-co-BT), and obviously the glass transition temperature of the blend significantly raises as the TA content in the blend is increased. Since TA is a polyphenolic molecule with a lot of hydroxyl groups, some of these hydroxyl groups as freely OH are not involved in either self-associated or inter-associated hydrogen bonding

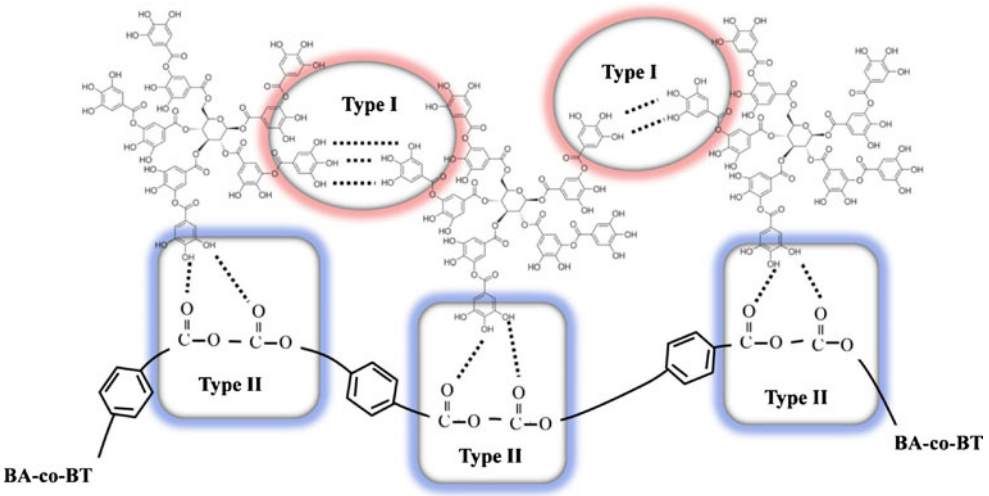


**Fig. 12** Interaction states of the miscible TA/P(BA-co-BT) blends in this study. The interaction state of Type I presents that the TA molecules are able to connect with each other by self-associated hydrogen bonding interactions. The interaction state of Type II exhibits inter-associated hydrogen bonds between TA and P(BA-co-BT), enabling the formation of miscible TA/P(BA-co-BT) blends

interactions. However, sufficient interactions between TA and P(BA-co-BT) can still result in the miscibility of TA/P(BA-co-BT) blends.

## Conclusions

The miscibility of biocompatible/biodegradable blends with specific interactions is important to their further applications and is addressed in this work. The miscibility of TA/P(BA-co-BT) as a biocompatible/biodegradable blend is studied by characterizing its phase morphology, thermal behavior and the interactions of its constituent components. The phase images of the blends preliminarily observed by OM show the homogeneous phase behavior. LCST behavior that might be induced by gradually elevating the temperature of the blends was also absent by careful detection of OM. High-resolution phase images for the blends were obtained by SEM, and all show a single phase cross-section for the blends without discernible phase domains, supporting the homogeneous phase behavior that was identified by OM. DSC experiments were performed to examine the thermal behavior that was associated with the miscibility of the blends. DSC thermal scans revealed a single $T_g$ for each of the compositions in the blends, indicating that the binary blends of TA/P(BA-co-BT) are miscible at all compositions. $T_g$-composition relationship was also analyzed and the Kwei equation fitted well when suitable parameters as $k=0.4$ and $q=85$ were used. These moderate values of k and q suggest moderate interactions between TA and P(BA-co-BT). In addition, decreasing $\Delta H_f$ on increasing the TA content was also presented, inferring the disruption of the crystallizing P(BA-co-BT) chains by the interacting non-crystalline TAs in the blends. FTIR was carried out to elucidate the interactions in the blends. Absorption regions that were related to the spectral characteristics of functional groups were resolved. According to the IR spectra, the absorption intensity of self-associated hydroxyl groups of TA gradually decreased as the P(BA-co-BT) content increased. Additionally, as the amount of P(BA-co-BT) in the blends increased, a low-frequency shift that was resolved from the phenolic stretching band of TA was presented. It reveals that the interactions such as the hydrogen bonding interactions occur as the P(BA-co-BT) content in the blends is increased. Analysis of the carbonyl stretching region also reveals spectral variation by changing the TA/P(BA-co-BT) blending ratio. The evidence that is provided by the IR spectral and related analyses suggests that intermolecular hydrogen bonds can occur in the binary blends of TA and P(BA-co-BT). Noisothermal crystallization of the blends was also found to be influenced by the hydrogen bonding interactions in the blends. With the presence of TA in the blends, the peak temperature of nonisothermal crystallization of P(BA-co-BT) was shifted to lower temperature, in addition, the heat of nonisothermal crystallization was also decreased. The amorphous TA in the blends could significantly retard and suppress the nonisothermal crystallization of crystalline P(BA-co-BT) due to their intimate mixing caused by the interactions as hydrogen bonds. The hydrogen bonding interactions between TA and P(BA-co-BT) are suggested as the main factor of the miscibility for TA/P(BA-co-BT) blends. These interactions lead to the formation of miscible blends of all TA/P(BA-co-BT) compositions, and to enhance the inter-mixing between TA and P(BA-co-BT). A novel blending system in a well-mixing/miscible state is developed herein. By sufficient and clear results of DSC, OM, SEM and FTIR, the miscibility and interactions of the TA/P(BA-co-BT) blends have been successfully characterized and proved. The combination of the biocompatible TA and the biodegradable P(BA-co-BT) make their blends versatile for advanced applications and biological or polymeric production end-uses. Introducing hydrogen bonding interactions is one effective way to ensure thorough mixing of constituents in the blends. The concept of introducing hydrogen bonds in the blends, no longer applied only to the conventional polymer or plastic blending systems, is expected to be exploited in novel systems such as the polymeric blends with biological functions.

**Acknowledgments** This work has been financially supported by basic research grants (NSC 101-2218-E-035-004-) from Taiwan's National Science Council (NSC), to which the authors express their gratitude.

## References

1. Bieligmeyer M, Taheri SM, German I, Boisson C, Probst C, Milius W, Altstädt V, Breu J, Schmidt H-W, D'Agosto F, Förster S (2012) J Am Chem Soc 134:18157
2. Huang YK, Jen TH, Chang YT, Yang NJ, Lu HH, Chan SA (2010) Acs Appl Mater Interfaces 2:1094
3. Liu JS, Chen M, Lu SF, Chen CH (2011) J Polym Res 18:1527
4. Lai CS, Ho CC, Chen HL, Su WF (2013) Macromolecules 46:2249
5. Kuo SW (2008) J Polym Res 15:459
6. Mori D, Benten H, Ohkita H, Ito S, Miyake K (2012) Acs Appl Mater Interfaces 4:3325
7. Lu HH, Ma YS, Yang NJ, Lin GH, Wu YC, Chen SA (2011) J Am Chem Soc 133:9634
8. Inganas O, Zhang FL, Andersson MR (2009) Accounts Chem Res 42:1731
9. Dimitrov SD, Bakulin AA, Nielsen CB, Schroeder BC, Du JP, Bronstein H, McCulloch I, Friend RH, Durrant JR (2012) J Am Chem Soc 134:18189
10. Huang H, Chen ZH, Ortiz RP, Newman C, Usta H, Lou S, Youn J, Noh YY, Baeg KJ, Chen LX, Facchetti A, Marks TJ (2012) J Am Chem Soc 134:10966
11. Faisant JB, Ait-Kadi A, Bousmina M, Deschenes L (1998) Polymer 39:533
12. Yilgor I, Bilgin S, Isik M, Yilgor E (2012) Polymer 53:1180
13. Vaynzof Y, Bakulin AA, Gelinas S, Friend RH (2012) Phys Rev Lett 108: doi: 10.1103/PhysRevLett.108.246605
14. Brenner TJK, Vaynzof Y, Li Z, Kabra D, Friend RH, McNeill CR (2012) J Phys D-Appl Phys 45: doi: 10.1088/0022-3727/45/41/415101
15. Pierre A, Lu SF, Howard IA, Facchetti A, and Arias AC (2013) J Appl Phys 113: doi: 10.1063/1.4801662
16. Gan Z, Kuwabara K, Yamamoto M, Abe H, Doi Y (2004) Polym Degrad Stab 83:289

17. Ishioka R, Kitakuni E, Ichikawa Y (2002) Polyesters III: applications and commercial products. In: Doi Y, Steinbüchel A (eds) Biopolymer vol 4. Weinheim, Germany, pp 275–298
18. Gruber P, O'Brien M (2002) Polyesters III: applications and commercial products. In: Doi Y, Steinbüchel A (eds) Biopolymer vol 4. Weinheim, Germany, pp 235–249
19. Aarar J, Gruys KJ (2002) Polyesters III: applications and commercial products. In: Doi Y, Steinbüchel A (eds) Biopolymer vol 4. Weinheim, Germany, pp 53–90
20. Kuwabara K, Gan Z, Nakamura T, Abe H, Doi Y (2002) Biomacromolecules 3:390
21. Cranston E, Kawada J, Raymond S, Morin FG, Marchessault RH (2003) Biomacromolecules 4:995
22. Jiang L, Wolcott MP, Zhang J (2006) Biomacromolecules 7:199
23. Lee LT, Woo EM, Chen WT, Chang L, Yen KC (2010) Colloid Polym Sci 288:439
24. Haslam E (1996) J Nat Prod 59:205
25. Edelmann A, Lendl B (2002) J Am Chem Soc 124:14741
26. Frazier RA, Papadopoulou A, Mueller-Harvey I, Kissoon D, Green RJ (2003) J Agric Food Chem 51:5189
27. Baxter NJ, Lilley TH, Haslam E, Williamson MP (1997) Biochemistry 36:5566
28. Yen KC, Mandal TK, Woo EM (2008) J Biomed Mater Res Part A 86A:701
29. Kuo SW, Chan SC, Chang FC (2002) Polymer 43:3653
30. Gordon M, Taylor JS (1952) J Appl Chem 2:493
31. Kwei TK (1984) J Polym Sci Polym Lett Ed 22:307
32. Coleman MM, Graf JF, Painter PC (1991) Specific interactions and the miscibility of polymer blends. Technomic, Lancaster
33. Woo EM, Chou YH, Chiang WJ, Chen IT, Huang IH, Kuo NT (2010) Polym J 42:391
34. Nurkhamidah S, Woo EM, Huang IH, Su CC (2011) Colloid Polym Sci 289:1563